Environmental Pollution 243 (2018) 1287–1301

Contents lists available at ScienceDirect

Environmental Pollution

journal homepage: www.elsevier.com/locate/envpol

Spatial variation of modelled total, dry and wet nitrogen deposition to forests at global scale

Donna B. Schwede [a, *], David Simpson [b, c], Jiani Tan [d], Joshua S. Fu [d], Frank Dentener [e], Enzai Du [f, g], Wim deVries [h, i]

[a] National Exposure Research Laboratory, U.S. Environmental Protection Agency, Research Triangle Park, NC, 27711, United States
[b] EMEP MSC-W, Norwegian Meteorological Institute, Oslo, Norway
[c] Dept. Space, Earth and Environment, Chalmers University of Technology, Gothenburg, Sweden
[d] Department of Civil and Environmental Engineering, University of Tennessee, Knoxville, TN, 37996, USA
[e] European Commission, Joint Research Centre, Ispra, Italy
[f] State Key Laboratory of Earth Surface Processes and Resource Ecology, Faculty of Geographical Science, Beijing Normal University, Beijing, 100875, China
[g] School of Natural Resources, Faculty of Geographical Science, Beijing Normal University, Beijing, 100875, China
[h] Wageningen University and Research, Environmental Research, PO Box 47, NL-6700 AA, Wageningen, the Netherlands
[i] Wageningen University and Research, Environmental Systems Analysis Group, PO Box 47, NL-6700 AA, Wageningen, the Netherlands

ARTICLE INFO

Article history:
Received 15 June 2018
Received in revised form
12 September 2018
Accepted 17 September 2018
Available online 20 September 2018

Keywords:
Nitrogen deposition
Dry deposition
Wet deposition
Forest biomes
Modelling approach

ABSTRACT

Forests are an important biome that covers about one third of the global land surface and provides important ecosystem services. Since atmospheric deposition of nitrogen (N) can have both beneficial and deleterious effects, it is important to quantify the amount of N deposition to forest ecosystems. Measurements of N deposition to the numerous forest biomes across the globe are scarce, so chemical transport models are often used to provide estimates of atmospheric N inputs to these ecosystems. We provide an overview of approaches used to calculate N deposition in commonly used chemical transport models. The Task Force on Hemispheric Transport of Air Pollution (HTAP2) study intercompared N deposition values from a number of global chemical transport models. Using a multi-model mean calculated from the HTAP2 deposition values, we map N deposition to global forests to examine spatial variations in total, dry and wet deposition. Highest total N deposition occurs in eastern and southern China, Japan, Eastern U.S. and Europe while the highest dry deposition occurs in tropical forests. The European Monitoring and Evaluation Program (EMEP) model predicts grid-average deposition, but also produces deposition by land use type allowing us to compare deposition specifically to forests with the grid-average value. We found that, for this study, differences between the grid-average and forest specific could be as much as a factor of two and up to more than a factor of five in extreme cases. This suggests that consideration should be given to using forest-specific deposition for input to ecosystem assessments such as critical loads determinations.

Published by Elsevier Ltd.

1. Introduction

The global nitrogen (N) cycle has been dramatically accelerated by anthropogenic activities since the industrial revolution, including an increase of atmospheric N emissions and a consequent enhancement of N deposition (Galloway et al., 2004, 2008). Forests cover approximately one third of the global land area and provide fundamental ecosystem services (Keenan et al., 2015). As an external nutrient input, N deposition often stimulates primary production and CO_2 sequestration in N-limited forest ecosystems (De Vries et al., 2006; Sutton et al., 2008; Högberg, 2012; Schulte-Uebbing and De Vries, 2018; Du and De Vries, 2018). However, with high levels of N deposition (above 15–25 kg N $ha^{-1}yr^{-1}$, De Vries et al., 2014a), the stimulating effect on forest growth likely diminishes over time due to accompanying side effects, such as soil acidification, imbalances between N and other nutrients such as phosphorous, calcium and magnesium, and increasing availability of toxic metals (e.g., aluminum) (Aber et al., 1998; Bowman et al., 2008; De Vries et al., 2014b; Du and Fang, 2014). Moreover, both N addition experiments in forest systems (e.g.

* Corresponding author.
E-mail address: Schwede.donna@epa.gov (D.B. Schwede).

https://doi.org/10.1016/j.envpol.2018.09.084
0269-7491/Published by Elsevier Ltd.

Skrindo and Økland, 2002; Strengbom et al., 2003; Nordin et al., 2006) as well as observational studies across N deposition gradients (e.g. Seidling et al., 2008; Van Dobben and De Vries, 2010, 2017; Dirnböck et al., 2014) showed significant effects of N deposition on the understory community, including a reduction in plant species diversity. In this context, there is an increasing need for high-resolution and timely updated mapping of N deposition to improve the understanding of its impacts on global forest biomes.

Continuous large-scale measurements of wet deposition have been routinely conducted by several regional monitoring networks (Dentener et al., 2014). Data from these networks as well as independent stations have greatly improved our understanding of spatial-temporal patterns of wet deposition in these regions (Vet et al., 2014). Dry deposition is usually estimated by multiplying the ambient concentrations of N-containing gas and particle species by their modelled dry deposition velocities. Large uncertainties in dry deposition remain due to incomplete measurements of N species and uncertainty in deposition velocities (Dentener et al., 2014). At a global scale, monitoring datasets are still lacking in many regions, especially in the southern hemisphere, and this hinders a global estimate of N deposition based on a spatial extrapolation of measurements. Atmospheric chemistry transport models are more comprehensive in that they estimate regional and global patterns of N deposition by simultaneously considering both wet and dry deposition processes, and are able to provide information in regions lacking monitoring. Existing modelling assessments of present-day N deposition are, however, outdated in view of rapidly changing N deposition inputs (e.g., year 1995 for Dentener et al., 2006; year 2000 for Lamarque et al., 2013; year 2001 for Vet et al., 2014; year 2010 for Tan et al., 2018), while simulations for more recent years are based on uncertain emission projections (e.g. Lamarque et al., 2013).

Differences in temporal and regional atmospheric deposition trends have been reported for oxidized and reduced N species (e.g., nitrate and ammonium). As a result of efforts to curb NO_x emissions, Europe and the U.S. have been experiencing a decrease in total N deposition since the middle 1990s, while reduced N has increased significantly, since there have been few programs targeting reductions in NH_3 emissions (Waldner et al., 2014; Du et al., 2014b; Du, 2016). However, total N deposition in China has increased dramatically from 1980 to 2010 due to increases in fertilizer use and the number of motor vehicles (Liu et al., 2013) and industries. Therefore, large areas of China's forests are exposed to high levels of N deposition (Du et al., 2014a; Du et al., 2016). Moreover, the components of reactive N (oxidized N + reduced N) do not result in the same biological and ecological effects. For instance, plants usually have a specific preference in utilizing soil ammonium or nitrate (Britto and Kronzucker, 2013), while ammonium can be more detrimental than nitrate by for decreasing plant biodiversity (Britto and Kronzucker, 2002). Therefore, it is necessary to separately consider oxidized and reduced N species when assessing N deposition across global forest biomes.

This study reviews available atmospheric chemical transport models at global and continental scales to estimate N deposition, including conceptual differences between the models, the role of measurement-model fusion approaches and the use of remote sensing. Furthermore, we present updated (base year 2010) global estimates of N deposition and its components (wet vs. dry, oxidized N vs reduced N) across forests biomes by using the HTAP2 multi-model ensemble (Tan et al., 2018). Using the EMEP MSC-W model (Simpson et al., 2006, 2012, 2017), particular attention is devoted to distinguishing grid-average and forest-specific deposition values in forested areas.

2. Overview of modelling approaches for estimating nitrogen deposition

2.1. Current monitoring and modelling efforts

Ecological assessments often require input of the loading of nutrients to the system. Wet deposition of reactive N is routinely monitored by various networks across the globe including the Acid Deposition Monitoring Network in East Asia (EANET; http://www.eanet.asia/index.html), European Monitoring and Evaluation Programme (EMEP; http://www.emep.int/), Canadian Air and Precipitation Monitoring Network (CAPMoN; (https://www.canada.ca/en/environment-climate-change/services/air-pollution/monitoring-networks-data/canadian-air-precipitation.html), and the U.S. National Atmospheric Deposition Program's National Trends Network (NADP/NTN; http://nadp.slh.wisc.edu/). Quality-controlled data from these networks as well as independent stations were used by Vet et al. (2014) in a global assessment of wet deposition. Vet et al. (2014) noted that wet deposition data are lacking in many areas of the world and that not all chemical species are measured at existing monitoring sites. Notably absent from most of the networks are measurements of wet deposition of organic N, which may contribute 20–30% of the total reactive N in precipitation (Neff et al., 2002; Kanakidou et al., 2016).

Dry deposition is not routinely monitored as direct measurements are difficult and expensive, particularly in forest ecosystems. Most networks that report dry deposition values, e.g. the International Global Atmospheric Chemistry Programme's Deposition of Biogeochemically Important Trace Species (IGAC/DEBITS), CAPMoN, and CASTNET use an inferential method (Wesely and Hicks, 2000) in which the measured atmospheric concentrations are multiplied by a modelled deposition velocity. These network values are determined for specific sites and are not easily extrapolated to provide a spatial coverage of dry deposition fluxes. Additionally, many dry deposition networks only measure the concentration of a subset of N species and often exclude one or more important chemical species such as NH_3, HNO_3, NO_2, and organic N components.

In addition to ground-based measurements, remote sensing technologies are increasingly used to obtain deposition estimates and offer the ability to provide improved spatial coverage of surface concentrations, particularly in areas where monitoring efforts are limited. Similar to dry deposition monitoring networks, an inferential method is used where satellite-based concentrations are paired with modelled deposition velocities to obtain the dry deposition fluxes. For instance, Kharol et al. (2018) used satellite data to compute fluxes of NH_3 and NO_2 over North America. Jia et al. (2016) used OMI satellite measurements supplemented with global ground-based measurements to estimate the dry deposition of reactive N compounds over a 10-year time period (2005–2014).

Regional and global atmospheric models offer the ability to obtain spatially continuous values of wet and dry deposition and typically include a more complete representation of the N budget than is available from monitoring networks. However, atmospheric models are subject to uncertainties in inputs including emissions and meteorology. By necessity, model parameterizations are often simplifications of real atmospheric processes, which results in additional uncertainty. Atmospheric models are continually being updated as new studies provide additional details on processes, but advancements are still slow (World Meteorological Organization, 2017). Of particular importance to the reactive N budget are recent studies that focused on the chemistry of organic N. These recent studies have shown that organic N can comprise 20–30% of the total N budget (Cornell et al., 2003; Cornell, 2011; Cape et al., 2011; Kanakidou et al., 2012; Kanakidou et al., 2016; Jickells et al.,

2013), but characterizing the explicit chemical species and partitioning between the gas and aerosol phases is challenging. In forest areas, the interaction between biogenic volatile organic compounds and NO_x can be an important pathway for the formation of organic nitrates (Ng et al., 2017; Pye et al., 2015), which then can be deposited. Models such as EMEP contain some limited treatment of the formation of organic nitrates (e.g. only PAN and isoprene-derived compounds) while others such as Community Multiscale Air Quality Model (CMAQ) have recently been updated to include more advanced treatment of organic N chemistry (Appel et al., 2017; Xu et al., 2018).

Recent efforts have sought to take advantage of the strengths of both the measurements and the models by combining them in a measurement-model fusion approach. The measurement data are used to bias adjust the modelled values and the modelled values provide additional detail in areas where monitoring sites are sparse. Schwede and Lear (2014) report on an approach used in the U.S. for obtaining values of total deposition of N and S for the contiguous U.S. where gridded modelled concentrations from CMAQ are bias adjusted using monitored data from the Clean Air Status and Trends Network (CASTNET). The bias adjusted concentration surface is then multiplied by the CMAQ deposition velocities to create the corrected grids of dry deposition fluxes for measured S and N species. For unmeasured species, the (uncorrected) CMAQ deposition value is used. The modelled dry deposition is combined with the measured wet deposition from NADP/NTN to obtain total deposition estimates. This Total Deposition (TDep) product is available from NADP (http://nadp.slh.wisc.edu/committees/tdep/tdepmaps/). A similar effort has been initiated in Canada, using the Atmospheric Deposition Analysis Generated by Optimal Interpolation (ADAGIO) approach (Environment and Climate Change Canada, 2018). The ADAGIO approach uses measured concentration and precipitation to adjust estimates from the Global Environmental Multi-scale - Modelling Air quality and CHemistry (GEM-MACH) model (Moran et al., 2010). The US and Canada efforts differ in the data sources used and the interpolation techniques. Based on these North American hybrid methods, an effort has been initiated to develop a measurement-model fusion approach to obtain global estimates of total deposition (World Meteorological Organization, 2017).

2.2. Approaches and uncertainties of nitrogen deposition modelling in chemical transport models

There are a large number of global atmospheric chemistry transport/climate models used to compute deposition fluxes and they vary in the treatment of atmospheric processes, chemical reactions, and calculation of wet and dry deposition. Several recent studies have looked at the range of deposition velocities, concentration and deposition values that are predicted by various models.

2.2.1. Variations in nitrogen dry deposition

Variations in dry deposition values predicted by chemical transport models (CTMs) result from differences in concentrations and deposition velocities. Flechard et al. (2011), with updates in Simpson et al. (2012), extracted deposition velocity models from several chemical transport models (CTMs) and used them in conjunction with measured concentration values from field sites to examine the variability in the predicted deposition of reactive N compounds for the ecosystems studied. The deposition velocity for HNO_3 is controlled mainly by the atmospheric stability, so inter-model differences in the deposition velocity were small in these studies. For other N compounds, however, variations in deposition velocities used in the models were a factor of 2 or greater, being mainly attributed to differences in the surface resistance. Using data from 14 regional-scale (grid sizes ranging from $0.25^\circ \times 0.25^\circ$–$0.25^\circ \times 0.4^\circ$) model simulations, executed as part of the Air Quality Model Evaluation International Initiative (AQMEII) and EURODELTA projects, Vivanco et al. (2018) presented an intercomparison and evaluation of N deposition. Measurements of dry deposition were not available for model evaluation but model intercomparisons showed considerable differences in the magnitude and spatial patterns of dry deposition. Model evaluation results were reported for the fractional bias in wet deposition with values ranging from −1.5 to 0.07 and −0.81 to 0.17 for $NO3^-$ and $NH4^+$, respectively, when annual values were considered. Simpson et al. (2014) examined the range of deposition values at the continental scale from four CTMs and found that while total N deposition values were similar between models, there were differences of about 30% in the wet and dry deposition. Greater differences were noted for individual N species. Tan et al. (2018) examined the deposition values from 11 global models that participated in the 2010 Task Force Hemispheric Transport of Air Pollution (HTAP2) study. Comparing total deposition of oxidized and reduced N, Tan et al. (2018) found total deposition values from the different models ranged from 15 to 26 Tg-N yr^{-1} globally and dry deposition of NH_3 ranged from 11 to 19 Tg-N yr^{-1}. Given the variations in deposition values shown by these studies, further research is needed to understand the underlying processes and improve and harmonize the parameterizations.

2.2.2. Treatment of resistances determining dry deposition velocity

The existing models used in previous studies vary in their treatment of dry deposition processes. To calculate the dry deposition of gases, most CTMs calculate a deposition velocity that is then multiplied by the concentration to obtain the flux. The deposition velocity (v_d) is usually calculated using the resistance framework

$$v_d = (R_a + R_b + R_c)^{-1}$$

where R_a is the aerodynamic resistance (s m^{-1}), R_b is the quasi-laminar boundary layer resistance (s m^{-1}), R_c is the canopy resistance (s m^{-1}).

For CTMs, R_a is typically calculated using similarity theory and is heavily dependent on the meteorology and the surface characteristics. The canopy resistance is also very dependent on the surface characteristics and is further broken down into component resistances including the vegetation (mesophyll, stomatal, and cuticular) and ground resistances. Models such as GEOS-Chem (Bey et al., 2001) and CHASER (Sudo et al., 2002) define the component resistances as in Wesely (1989). EMEP uses the approach of Emberson et al. (2001) and is extended for other gases as in Simpson et al. (2012, 2017). GEM-MACH uses the approach of Zhang et al. (2003) and CMAQ uses the framework of Pleim and Ran (2011). These four approaches use a similar multiplicative formulation (e.g. Jarvis, 1976) for the stomatal resistance, but vary considerably in their treatment of the cuticular and ground resistances. Another common approach for calculating stomatal resistance is to link the stomatal uptake to the photosynthetic processes as in CAM-Chem (val Martin et al., 2014). In addition, some models have special considerations for the deposition of NH_3. The EMEP model uses a co-deposition approach in which non-stomatal deposition rates depend on an 'acidity ratio', $[SO_2]/[NH_3]$, as well as relative humidity and temperature; deposition of NH_3 is for example higher in areas with high acidity ratios and/or high humidity. In a crude accounting for bi-directional exchange, ammonia deposition to crops (which are often sources rather than sinks of NH_3) is set to zero in EMEP while CMAQ contains a more explicit approach to determine the stomatal and soil compensation

points which determine the bidirectional flux of NH_3 (Bash et al., 2013). Similar explicit approaches are beginning to be included in other CTMs such as LOTOS-EUROS (Wichink Kruit et al., 2012). Bi-directional exchange may impact all deposition estimates to some extent, but is most important in areas in and close to NH_3 sources (e.g. agricultural areas). In such areas, emissions of NH_3 are possible when ambient NH_3 is low. In most forested areas, however, there are no major sources of NH_3, and deposition rates should be given adequately by standard uni-directional deposition approaches. Some exceptions to this assumption have been observed, e.g, Hansen et al., 2013 found large emissions of NH_3 from deciduous forests after leaf fall, but this was over a limited period from a region which experiences high N-deposition loads. In tropical forests, the extensive biodiversity presents additional challenges in predicting the direction of NH_3 exchange as emission potentials will vary widely with plant species and forest litter (Hedin et al., 2009). Additional experimental work is needed to improve the understanding of processes controlling the deposition of gases, particularly the surface resistances and the role of leaf litter.

Dry deposition of aerosols is also typically modelled using a resistance framework and often builds on the work of Slinn (1982) with parameterizations of the form

$$v_d = (R_a + R_s)^{-1} + v_g$$

where R_a is the aerodynamic resistance (s m^{-1}), R_s is the surface resistance (s m^{-1}), and v_g is the gravitational settling velocity (s m^{-1}). The surface resistance is parameterized to consider the collection efficiency of the aerosols due to various processes including Brownian diffusion, inertial impaction, interception by the vegetation, electrophoresis, and thermophoresis. Similar to gases, the deposition velocity is sensitive to the meteorology and the surface characteristics but also the particle size. Petroff et al. (2008a) and Pryor et al. (2008) provide extensive reviews of modelling approaches currently used in atmospheric models. Models differ in the treatment of the collection efficiency, with some models including more components (e.g. interception, thermophoresis) than others. The extent to which different resistances and collection efficiencies are important varies with the size of the aerosol. New approaches for calculating the dry deposition of aerosols have recently been proposed including those by Petroff et al. (2008b), Petroff and Zhang (2010), Kouznetsov and Sofiev (2012), Zhang and He (2014), and Zhang and Shao (2014). Khan and Perlinger (2017) provide an evaluation of 5 aerosol deposition parameterizations and found that model performance was sensitive to the particle size and land use. Since the deposition velocity is size dependent, differences in deposition flux between CTMs will also depend on the characterization of the phase of the pollutant (depending on relative humidity) and the size of the particle as predicted by the variety of aerosol modules in global models. There are also suggestions that dry deposition rates for aerosols are much higher in unstable atmospheric conditions than given by models, for reasons which are not fully understood (Fowler et al., 2009). Continued research is needed to improve the understanding of aerosol deposition processes.

2.2.3. Treatment of wet deposition

Wet deposition parameterizations in CTMs typically consider in-cloud and below-cloud (rain/snow) scavenging. Vet et al. (2014) provide an assessment of global precipitation and wet deposition predicted by models as part of the HTAP project (Dentener et al., 2006). There are many differences between the meteorological and chemical transport models in terms of their ability to predict clouds and precipitation rate, type and intensity as well as the aqueous chemistry associated with clouds. Most models use Henry's Law to specify the solubility of gaseous pollutants and, for some components, an effective Henry's law coefficient that takes pH dependent dissociation (i.e. for SO_2) into account. A review of the range of Henry's law values for many chemicals is provided in Sander (2015). Recently, consideration of kinetic mass transfer that accounts for the diffusion across the air/water interfacial surface has been added to aqueous chemistry modules (Fahey et al., 2017). The in-cloud scavenging of aerosols depends on the effective nucleation of cloud droplets. Below-cloud scavenging is dependent on raindrop and particle size, as well as the evaporation of rain. Zhang et al. (2013) and Wang et al. (2010) present reviews of scavenging coefficients for below cloud scavenging of aerosols. Wang et al. (2010) found that values for the scavenging coefficient could vary by a factor of 3–5 due to the parameterization of the raindrop size distribution alone and that, when combined with uncertainties in the parameterization of the collection efficiency and other factors, the scavenging coefficient could differ by an order of magnitude across parameterizations.

2.2.4. Characterization of the land surface

In the descriptions of the major aspects of the deposition calculations provided above, the characterization of the land surface is an important model sensitivity. The land cover determines the leaf area index, surface roughness, canopy height, stomatal response, biogenic emissions, bidirectional NH_3 exchange and many other variables. A recent study demonstrated that analyses utilizing outputs of grid-cell averaged biomass rather than that of detailed PFT (plant function type)-level biomass resulted in larger biases of extratropical forest biomass simulated by Earth System Models (Yang et al., 2018). Biases in biomass values are also important in CTMs since these biases alter the heat, water, and carbon fluxes between the atmosphere and the land. Different atmosphere-land fluxes result in different regional meteorological conditions and thus increase the uncertainty of CTMs results. There are a number of different land cover data sets available for use with CTMs with varying levels of detail. Data sets do not exist that provide clear global values of LAI, surface roughness and other parameters based on vegetation type, season and latitude. These values are specified by the individual models and are often not validated for a wide range of biomes. It is unclear whether any work has been done in multi-model studies to harmonize the surface characteristics used by the models. CTMs use gridded representations of the land cover types and the surface characteristics. It is expected that the heterogeneity of the land cover in the grid will increase with the grid size. Some models use only the dominant land use category within a grid cell. Many models such as EMEP, GEM-MACH, GEOS-Chem and others, however, make use of the mosaic of land use types within the grid cell by calculating the deposition velocity to each land use type, which is weighted by the area to obtain the deposition velocity and/or fluxes for the grid cell. Other models, such as CMAQ, use a blended approach where surface characteristics are blended for the grid cell in the land surface model and the stomatal resistance for water vapor and the R_a for the grid cell are passed to the chemical transport model for use in calculating the deposition velocity for the grid cell. Flechard et al. (2011) and Simpson et al. (2014) compared the deposition velocity predicted by different models for a range of land use types and found that, for some chemical species, the deposition to a forest can be a factor of 2 or more greater than the deposition to grassland or crop areas, thus illustrating the importance of consideration of sub-grid land use type. Bidirectional exchange of ammonia, which is included in some chemical transport models, also varies with land cover type as the canopy and soil compensation points can be quite different across vegetation types as emission potentials can vary over several orders of magnitude (Massad et al., 2010). Since this analysis is

Table 1
Total deposition of NH_x-N, NO_y-N and total N on global forests using different criteria in assessing the area of forests (different cut-off points of forest coverage within an 18.5 × 18.5 km^2 grid). All data are based on an overlay of the Global Forest Monitoring Project data and the deposition at 1° × 1° in 2010, as calculated with HTAP[a] multi-model mean results.

Forest cover	Area (Million km^2)	NH_x-N dep (Tg N yr^{-1})	NO_y-N dep (Tg N yr^{-1})	Total N dep (Tg N yr^{-1})	Average N dep[b] (kg N ha^{-1} yr^{-1})
>1%	32.3	9.3	10.2	19.5	6.0
>5%	32.2	9.2	10.1	19.3	6.0
>10%	31.5	8.9	9.8	18.7	5.9

[a] The HTAP emissions inventory was provided at a resolution of 0.1° × 0.1° but the spatial resolutions of the underlying HTAP global models were coarser, being mostly in the order of 1° × 1°.
[b] Average N deposition was derived by dividing the total N deposition by the area.

Table 2
Total deposition of NH_x-N, NO_y-N and total N on worlds terrestrial ecosystems for the year 2010. All data are based on an overlay of the Global Land Cover map (GLC 2000) and HTAP multi-model ensemble results, averaged at 1° × 1°.

Land use class	Area (Million km^2)	NH_x-N (Tg N yr^{-1})	NO_y-N (Tg N yr^{-1})	Total N (Tg N yr^{-1})	Average N inputs[1] (kg N ha^{-1} yr^{-1})
Forest	42.9	10.3	12.3	22.5	5.3
Semi natural vegetation/grassland	44.5	9.6	9.6	19.2	4.3
Croplands	18.6	13.5	9.7	23.2	12.5
Other land	24.5	2.1	3.4	5.4	2.2
Total	130.6	35.4	35.0	70.3	5.4

concerned with total N deposition to forests, we examine the potential impact, on a global scale, of using forest-specific deposition values rather than grid-average deposition values on critical loads.

3. Modelled reactive nitrogen deposition to global forests

3.1. Modelling approach

We used two different modelled estimates for wet, dry and total deposition of NH_x (NH_3 + aerosol NH_4^+), NO_y (e.g. NO_2, HNO_3, N_2O_5, HONO, PAN and other organic nitrates, and aerosol NO_3^-) and total N deposition to forest biomes across the globe. The first is the multi-model mean (MMM) deposition at the grid scale from an ensemble of global deposition models used in the HTAP2 project (Tan et al., 2018). For HTAP2, 20 models were run using a common emissions platform based on a compilation of different regional gridded inventories for the USA, Canada, Europe, China, India and other Asian countries and gap-filled with the emission grid maps of the Emissions Database for Global Atmospheric Research (EDGARv4.3) for the rest of the world (mainly South America, Africa, Russia and Oceania). Details of the regional gridded inventories are given in Janssens-Maenhout et al. (2015) and Galmarini et al. (2017). The HTAP2 model MMM deposition was derived from 11 models used in the HTAP2 study that provided sufficient information on deposition. These models included CAM-Chem (Tilmes et al., 2016), CHASER_re1 (Sudo et al., 2002), CHASER_t106 re1 (Sudo et al., 2002), EMEP_rv48 (Simpson et al., 2012), GEM-MACH (Moran et al., 2010), GEOS5 (Rienecker et al., 2008; Colarco et al., 2010), GEOSCHEMAJOINT (Henze et al., 2007), OsloCTM3v.2 (Søvde et al., 2012), GOCARTv5 (Chin et al., 2000), SPRINTARS (Watanabe et al., 2010; Takemura et al., 2005) and C-IFS_v2 (Flemming et al., 2015). The model descriptions and configurations are introduced in Galmarini et al. (2017) (Table 3) and Stjern et al. (2016) (Table 1). Two criteria were used to screen models for inclusion in the MMM. First, values of deposition were compared against emissions. Only models having deposition values within ±20% of the emissions were included. Second, models were compared against the mean value from all of the models. Models were only included when they deviated from the multi-model mean by less than ±1.5 times the interquartile. The HTAP2 emission inventory was provided at a resolution of 0. 1° × 0.1°, but the spatial resolutions of the underlying HTAP2 global models were model specific, ranging from 0. 5° × 0.5°–2.8° × 2.8°. Output from the resulting 11 models was interpolated to a common 1° × 1° grid, and the arithmetic mean was calculated for each chemical species to create the MMM values. The model ensemble performances have been evaluated in Tan et al. (2018) for wet deposition (Figs. 1–2) and dry deposition (Figs. 3–4). The individual model performances are shown in Figs. S2-S11 in the supplementary of Tan et al. (2018).

The second data set used in this study is from the EMEP MSC-W model (Simpson et al., 2006, 2012, 2017, 2018), which was run at a global scale at 1° × 1° resolution. Version rv4.17 of the model was used for this study, similar to that utilized in Mills et al. (2018) and Stadtler et al. (2018). The model uses a mosaic approach for deposition, in which all land-cover types within a grid are treated separately and uses similarity theory for calculating the sub-grid atmospheric resistance values (Simpson et al., 2012). This makes deposition dependent on vegetation characteristics such as canopy height, LAI, or stomatal conductance, and deposition rates to forests are typically much greater than to low vegetation such as

Table 3
Total deposition of NH_x-N, NO_y-N and total N on global forest biomes (topical, subtropical, temperate and boreal) based on an overlay of the Global Forest Monitoring Project data and the deposition at 1° × 1° in 2010, as calculated with EMEP rv4.17 model, based on forest-specific values (first value) and grid-average values (value in brackets) in areas with >5% forest cover.

Forest biome	Area (Million km^2)	NH_x-N dep (Tg N yr^{-1})	NO_y-N dep (Tg N yr^{-1})	Total N dep (Tg N yr^{-1})	Average N dep[a] (kg N ha^{-1} yr^{-1})
Total	32.2	11.9 (10.8)	11.1 (9.8)	23.0 (20.6)	7.1 (6.4)
Tropical	16.9	6.1 (5.6)	6.1 (5.5)	12.1 (11.1)	7.2 (6.6)
Subtropical	3.5	3.1 (2.8)	1.9 (1.7)	5.1 (4.5)	14.6 (13)
Temperate	7.2	2.5 (2.1)	2.7 (2.3)	5.2 (4.4)	7.3 (6.2)
Boreal	4.6	0.2 (0.2)	0.3 (0.3)	0.6 (0.5)	1.2 (1.2)

[a] Average N deposition was derived by dividing the total N deposition by the area.

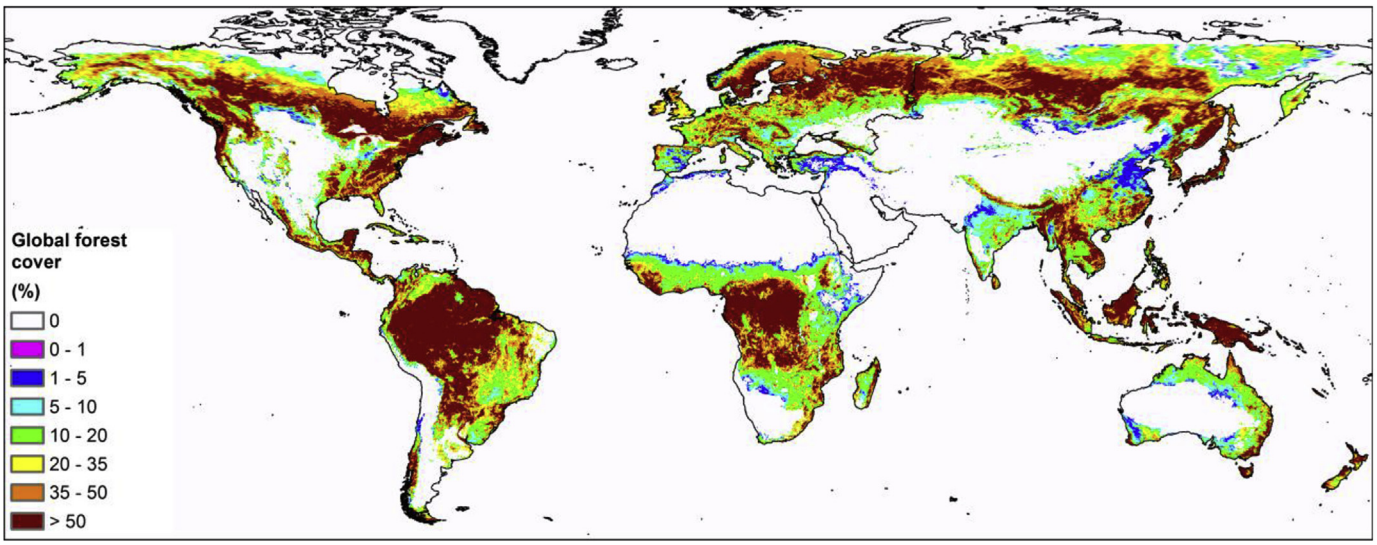

Fig. 1. Global forest coverage (%) in 18.5 × 18.5 km^2 grid cells based on the Globcover data (http://due.esrin.esa.int/page_globcover.php).

grasslands. Anthropogenic emissions are from the ECLIPSE data set (http://www.iiasa.ac.at/web/home/research/researchPrograms/air/ECLIPSEv5a.html, Klimont et al., 2017). Biogenic emissions of isoprene and terpenes are calculated in the model as described in Simpson et al. (2012, 2017). Soil and lightning NO are specified from external datasets (see Simpson et al., 2012). The EMEP model was also used in the HTAP2 MMM, however version EMEP rv4.8 was included in that study and HTAP2 emissions were used.

Values of deposition of NH_x and NO_y from the two data sources (MMM, EMEP) on a 1° × 1° lon-lat grid for the year 2010 were projected to an equal area (18.5 × 18.5 km^2) (ALBERS) projection. The resulting spatial map of global N deposition was combined with a global forest cover map for the year 2000 from the Global Forest Monitoring Project (https://glad.umd.edu/projects/gfm/global/gindex.html). This map is produced by calibrating MODIS-derived forest cover extent with Landsat data and details the extent of individual biomes. Forests were defined as areas with tree canopy coverage greater than 25% at the Landsat pixel scale (30 m × 30 m spatial resolution) for trees >5 m in height. (Hansen et al., 2010). Fig. 1 shows the forest coverage over the world. The distribution of forests by biome is provided in the Supplemental Information (SI) (Figure S1). Detailed information on land cover data used as input to the models in HTAP2 are not available and likely vary among the models. The EMEP MSC-W model uses a combination of European fine scale data, global landcover data from GLC-2000 (http://bioval.jrc.ec.europa.eu/products/glc2000/glc2000.php), and data from the Community Land Model (Oleson et al., 2010) as described in Simpson et al. (2012, 2017). Future studies should look at harmonization of land cover representations used for modelling and analysis.

3.2. Average total, dry and wet deposition of nitrogen compounds to grid cells

A comparison of the global scale deposition data for NH_x, NO_y and total N to forests, as calculated with the HTAP2 MMM, using different criteria for assessing the area of forests (different thresholds of forest cover within an 18.5 × 18.5 km^2 grid) is given in Table 1. Results show that there is little difference in the results for a threshold of 1% compared to 5%. However, the differences between

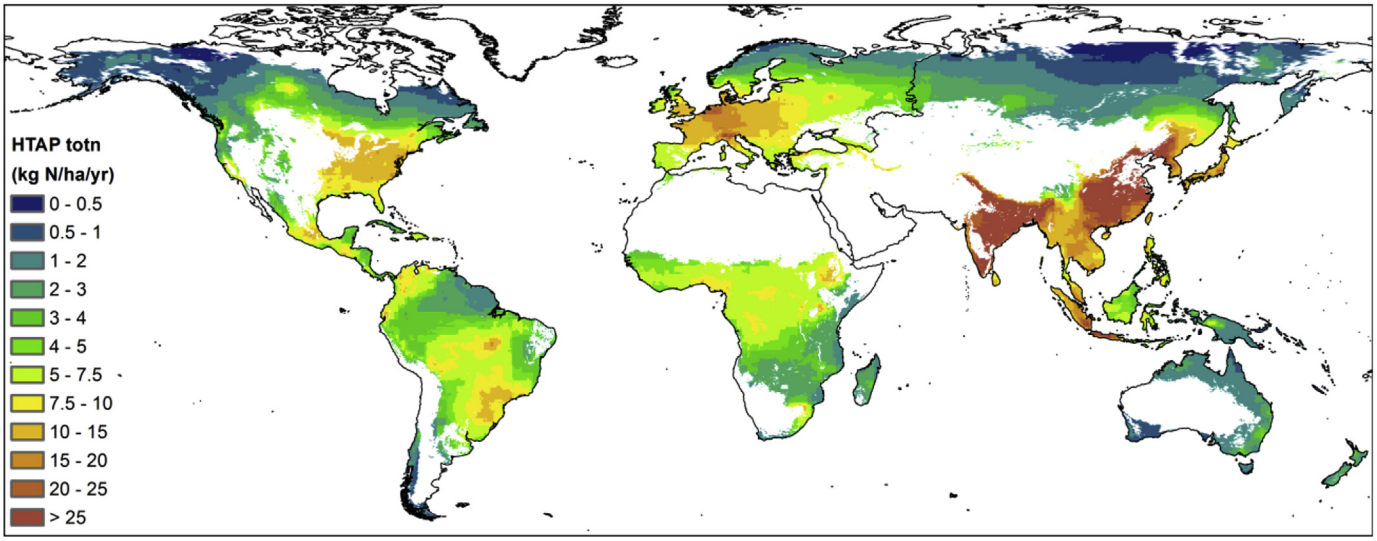

Fig. 2. Multimodel mean total N deposition (kgN ha^{-1}yr^{-1}) from the HTAP2 project on grid cells with a forest cover >5%.

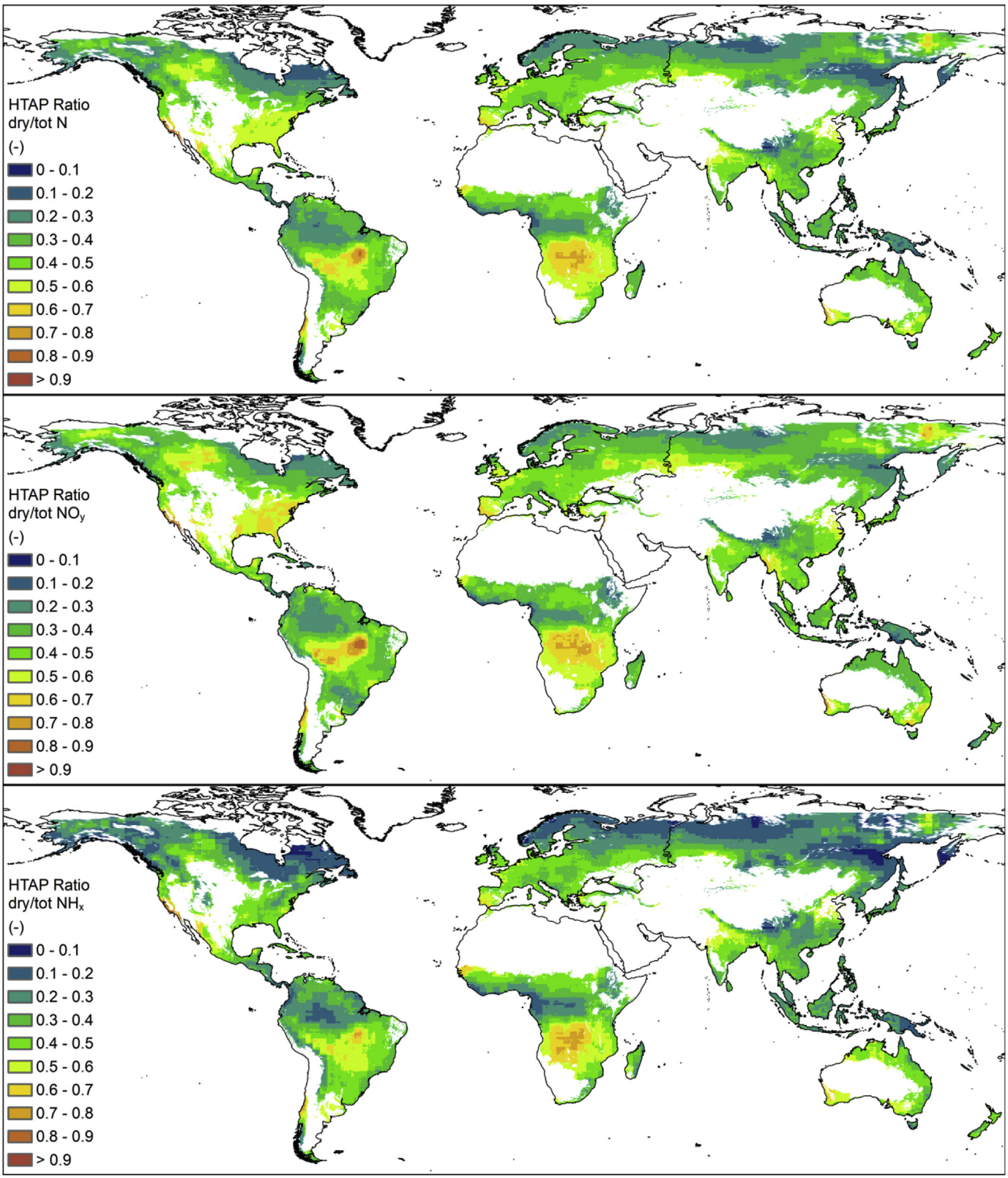

Fig. 3. Contribution of dry deposition to total deposition at grid level for total N (top), NO_y (middle) and NH_x (bottom) based on HTAP II multi-model model results.

a threshold of 5% and 10% are important, indicating the need to account for the smaller forests in our analysis. The areas with 5%–10% forest coverage account for a small area mostly located in East and Southeast Asia that have higher N deposition which increases the average global grid-based deposition. For the analyses presented here, we used a threshold of 5% forest cover to delineate forested areas. It should be noted that CTMs do not spatially resolve the location of subgrid landcover types within a grid cell and only

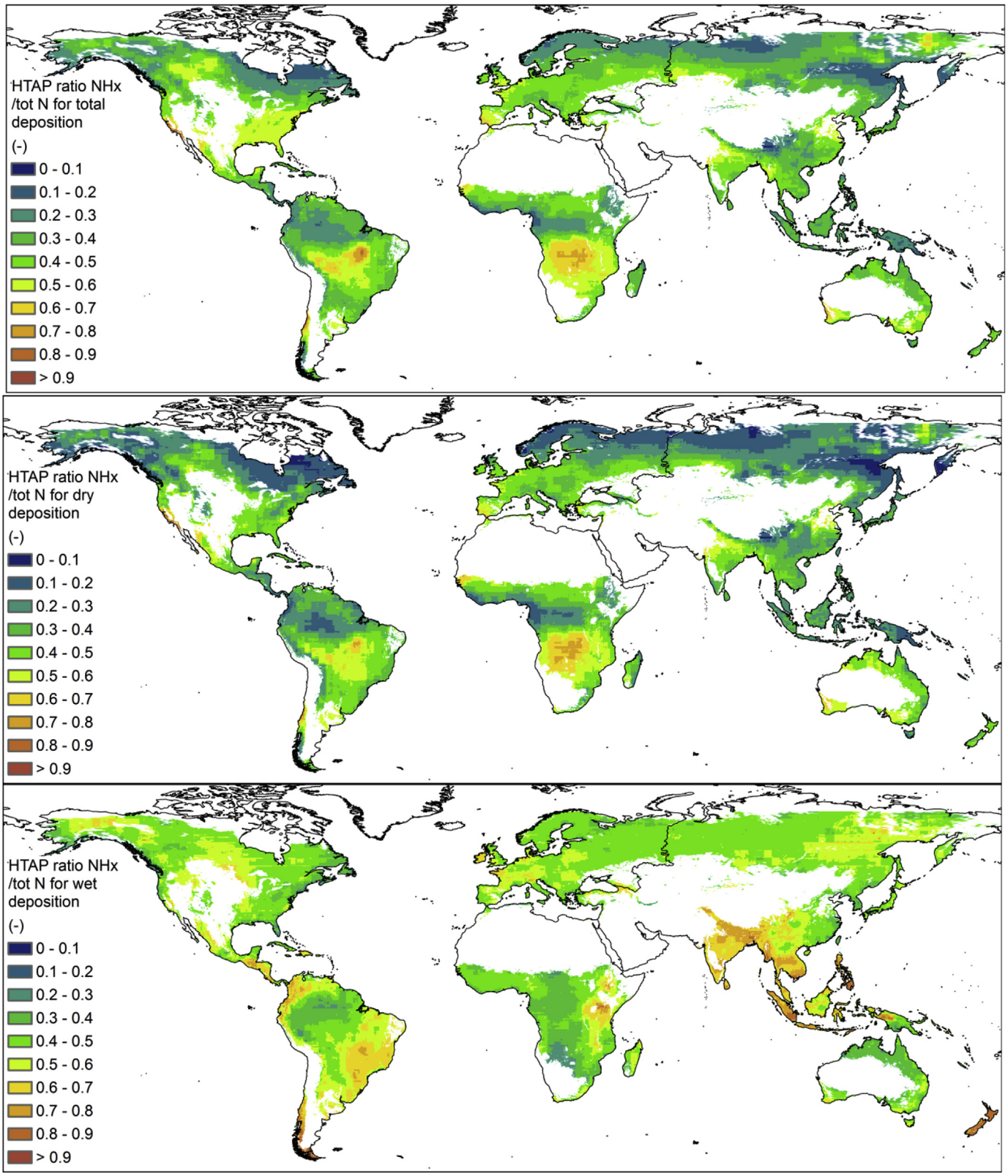

Fig. 4. Contribution of NHx deposition to total deposition (top), dry deposition (middle) and wet deposition (bottom) based on the HTAP II multi-model mean results.

use the percent coverage of the land use type within the grid cell. Fine scale exchange processes that might occur in reality, such as effects of the edges of forests or interactions between two adjacent land use types, are not modelled.

Globally, the average rate of total N deposition to forests is about 6 kg N ha^{-1} yr^{-1} and the total N input from atmospheric deposition is about 19 Tg N yr^{-1}. Oxidized N (NO_y) contributes slightly more to the total N than reduced N (NH_x) on a global basis (Table 1). To put

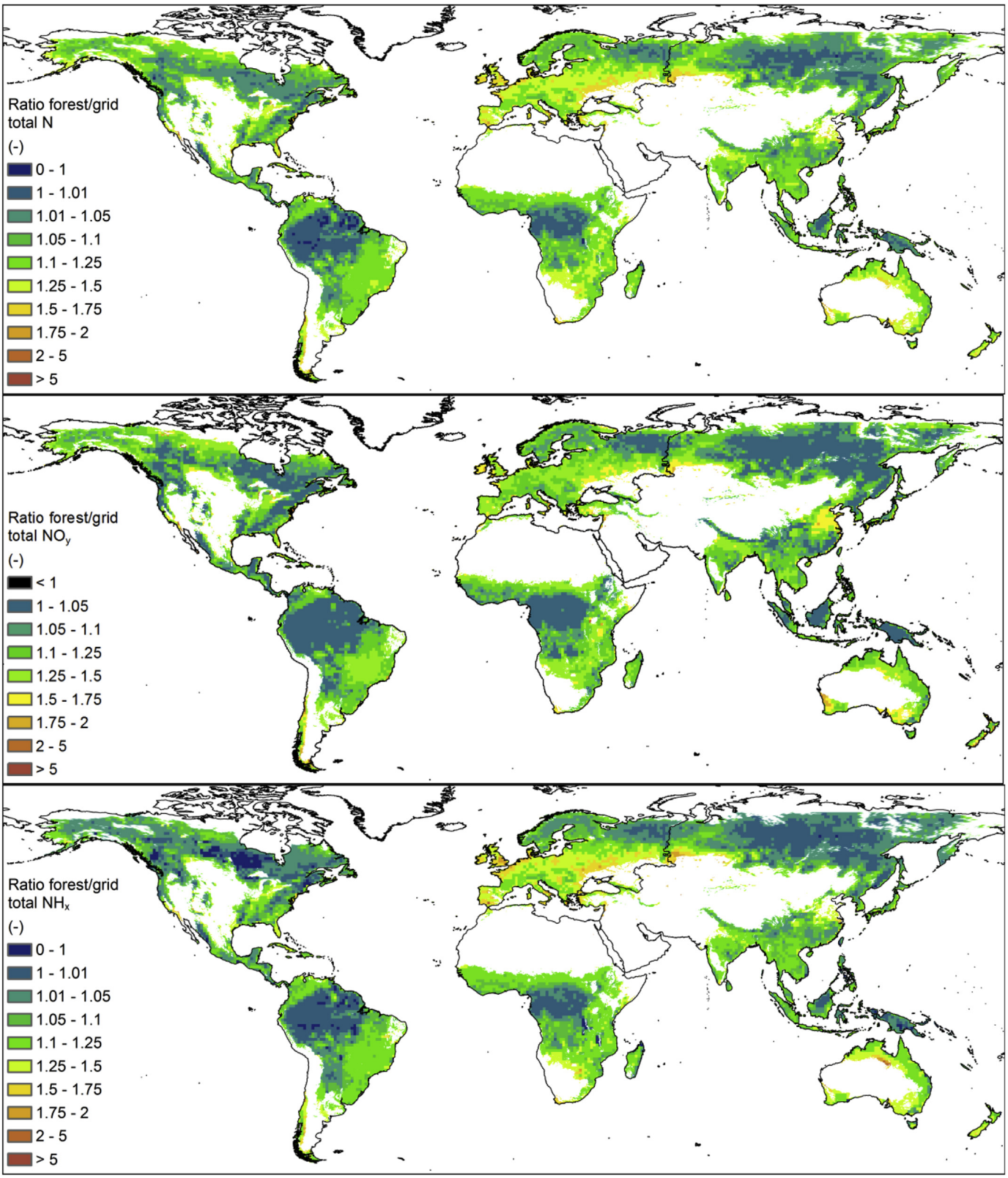

Fig. 5. Ratio of the forest-specific deposition to grid cell average deposition by the EMEP model for total deposition of total N (top), NO_y (middle) and NH_x (bottom).

the results for global forests into perspective with respect to other land uses, Table 2 presents information on the total deposition of NH_3, NO_x and total N all over the word, distinguishing between forests, semi natural vegetation (mainly grasslands), croplands and other land (bare land, urban areas). Results are based on an overlay of HTAP multi-model ensemble results with the Global Land Cover map (GLC 2000) at $1^\circ \times 1^\circ$ resolution. Results show that the computed N global deposition fluxes to forests is 32% of the global

deposition of N, while the percentage for the other land uses is 27% for semi natural vegetation/grasslands, 33% for croplands and 8% for other land. The percentages are (slightly) different when considering reduced and oxidized N species separately. As to be expected, the contribution of reduced N deposition to given land uses as compared to the global deposition of N is higher for croplands (where NH_3 is mainly emitted), i.e. 38%, and lower for remote areas, such forests and (bare) other land, i.e. 29% and 6%, respectively, in view of the comparatively short residence times in the atmosphere. Inversely, the contribution of oxidized N deposition is lower for cropland, i.e. 28%, and higher for forests, i.e. 35% (See Table 2). Note that the estimated total deposition to forests is higher in Table 2 as compared to Table 1 due to the coarser schematization of forests in the Global Land Cover map as compared to the global forest cover map.

A global map of the total deposition of N (kg N ha^{-1} yr^{-1}) to grid cells with a forest cover >5% is shown in Fig. 2. Total reactive N deposition is highest for forests in China, Japan, Indonesia, and India as well as in Eastern United States and in areas in central Europe. Lower deposition values are found in Western Canada and in Russia. To understand the spatial variability in total N, it is helpful to look at the spatial patterns of ratios of wet versus dry deposition and oxidized versus reduced N deposition. Maps of absolute deposition values as derived from HTAP2 MMM are provided in the SI (Figures S2-S4).

Fig. 3 shows the contribution of dry deposition to the total deposition for total N, NO_y and NH_x. The contribution of dry deposition to total N is highest in the tropical forests of central South America and central Africa (Fig. 3 top). This is likely due to the high LAI which provides increased surface area for deposition, long growing seasons, and high stomatal conductances in these areas, but also the relatively strong contribution of biomass burning in the dry season to the pollutant emissions. In Fig. 3 middle, we see that dry deposition of NO_y contributes more than wet deposition of NO_y in these same areas (South America and central Africa) as well as the eastern part of the US. The importance of NO_y dry deposition in the US is driven not only by LAI, but also NO_x emissions from industrial and mobile sources (Jiang et al., 2018). For NH_x deposition (Fig. 3 bottom), wet deposition dominates in the boreal forest areas while dry deposition dominates in the tropical forest regions. Additionally, there is a high contribution of dry deposition to total NH_x deposition in south central Africa, the west coast of the US, and a few isolated areas of South America. It should be noted that the models used in the HTAP2 study did not consider the bidirectional flux of NH_3. Models that do include bidirectional exchange may produce different spatial patterns from those shown here depending on the relative magnitudes of the air concentration and the canopy compensation points.

In Fig. 4, we examine the relative contributions of NO_y and NH_x to the total, dry and wet deposition. Considering total deposition (Fig. 4 top), NHx contributes greater than 60% and as much as 90% to the total N budget in the broad tropical forest areas of central South America and central Africa, whereas NO_y deposition contributes more than 70% in the northern boreal forests in Canada and Russia. The boreal forests also show a strong contribution of NO_y deposition in the dry deposition budget, as do some small areas in central South America and central Africa (Fig. 4 middle). The dry deposition to temperate forests is also mostly due to NO_y deposition but the fraction is lower. For wet deposition (Fig. 4 bottom), NH_x deposition exceeds NO_y deposition in the tropical forests of Central America, India, and southeastern Asia while other topical forests in central Africa and South America have a higher fraction of NO_y deposition.

The spatial patterns of deposition result from a combination of factors including emissions, meteorology and land cover. These patterns help identify potential sources and sinks of N across the forest types. A more detailed source apportionment study would be able to refine the analysis, but is beyond the scope of this overview study.

3.3. Comparison of forest-specific nitrogen deposition with grid cell average nitrogen deposition

The HTAP2 MMM only provides information on grid cell-average dry deposition. Deposition to individual land cover types within a grid cell can be quite different, with deposition velocities to forests typically being higher due to the higher LAI and canopy height. This was demonstrated in Flechard et al. (2011) as shown in Figure S5. The EMEP model sub-grid deposition module produces output of deposition by land cover type. We use the results from this model to explore the differences between estimates of global deposition from grid cell average values and forest-specific values.

The global scale deposition data for NH_x-N, NO_y-N and total N to different global forest biomes (tropical, subtropical, temperate and boreal) as calculated with EMEP rv4.17, based on grid cells with >5% forest cover is given in Table 3 and Table S1. As expected, total N deposition to all forests is higher by 12% when the forest-specific values are used (23.0 Tg N yr^{-1}) compared to the grid-average values (20.6 Tg N yr^{-1}). Table 3, also allows comparison of global deposition to the different forest biomes. The highest grid-average total deposition rate is to subtropical forest areas with a value of 13 kg N ha^{-1} yr^{-1}, but tropical forests account for the largest portion of the global total N deposition due to their large coverage area. The EMEP global total N deposition in 2010 for subtropical and temperate forests is similar with grid-average values of 4.5 and 4.4 kg N ha^{-1} yr^{-1} and of forest specific values 5.1 and 5.2 kg N ha^{-1} yr^{-1}, respectively. However, the contributions of reduced and oxidized N are quite different with reduced N deposition exceeding oxidized N deposition in subtropical forests with the reverse being the case for temperate forests. The temperate forests tend to be closer to more urbanized area and more exposed to emissions of NO_x.

Figs. 5 and 6 provide information on the spatial variability of the ratio of forest-specific deposition to the grid-averaged value for total deposition and dry deposition, respectively. Again, results are presented for all grid cells with >5% forests. Plots of absolute deposition are provided in the SI (Figures S6-S12). The spatial patterns of the ratios of forest-specific deposition to grid cell average deposition are overall very similar for total N, NO_y and NH_x (Fig. 5), but do have some important differences. For total N deposition, the areas that are densely covered with forests such as the northern part of South America, central Africa, and the boreal forest region in Russia have very low ratios as the grid cells are predominantly forest and the grid cell value is close to the forest-specific value (Fig. 5 top). In northern China, there is an area of small forest (cover < 10%) where the differences between the grid value and forest-specific value are high. In Western Europe and the United Kingdom, the forest coverage is typically 10–20% and the deposition ratio is > 1.5 indicating that the heterogeneity of the land cover is important. For NH_x deposition (Fig. 5 bottom), the differences between the grid-based value and the forest-specific value are lower in the temperate and boreal forests of Canada compared to the NO_y deposition (Fig. 5 middle), and there are some areas of Canada and Africa where the ratio is less than 1 (discussed further below). It is important to note that no consideration is given to any sub-grid variability in wet deposition and emissions in the models. Since total (wet + dry) deposition is presented in Fig. 5, the signal of the forest-specific deposition is masked in some areas by the wet deposition which does not vary at the sub-grid scale in EMEP. Wet deposition values for the grid cells are provided in

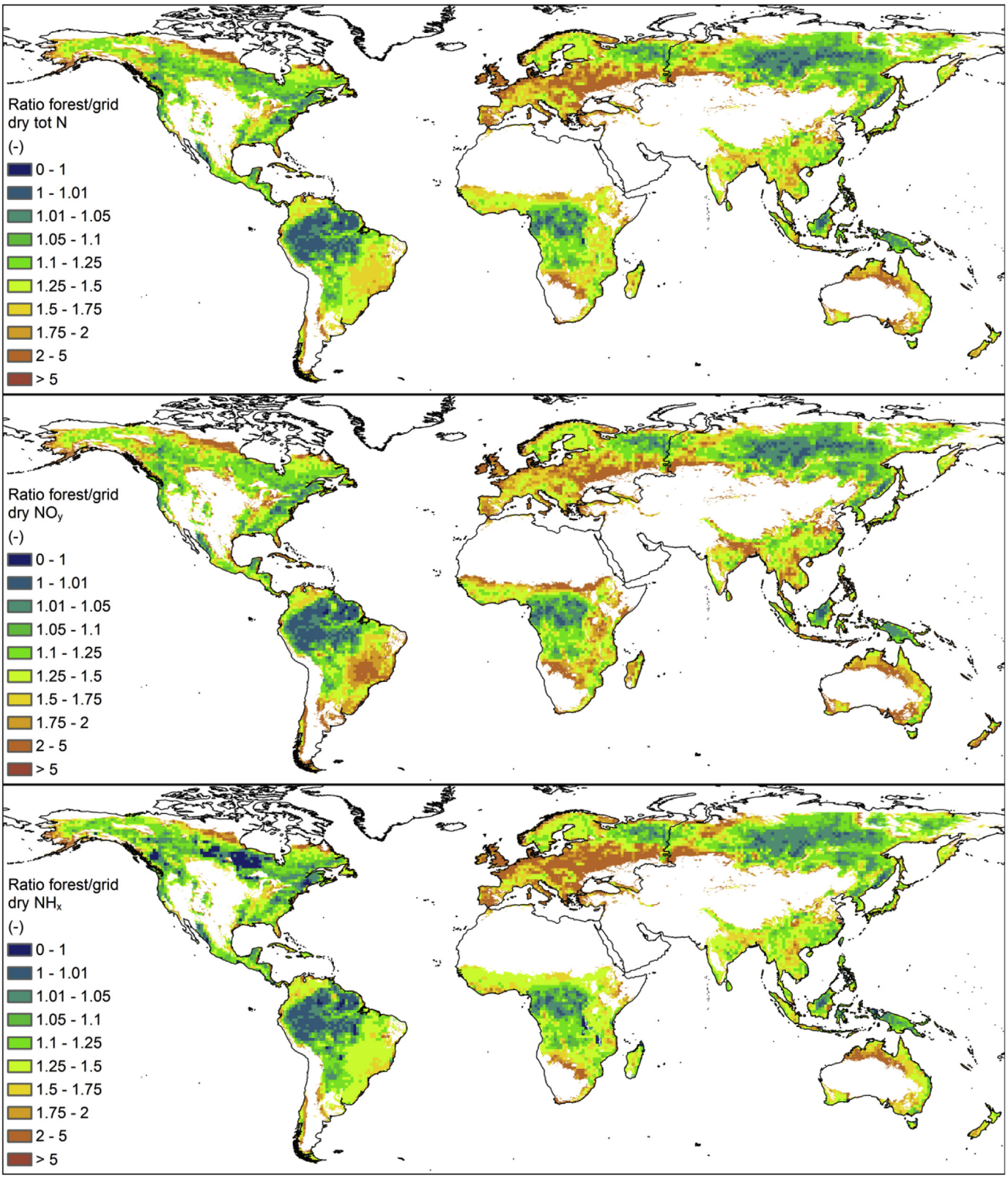

Fig. 6. Ratio of the forest-specific deposition to grid cell average deposition by the EMEP model for dry deposition of total N (top), NO_y (middle) and NH_x (bottom).

Figure S12 for comparison with the dry and total deposition values.

Fig. 6 focuses on dry deposition only and allows us to examine the impact of the sub-grid variability on deposition velocities. There is much more spatial variability in the ratios for dry deposition than for total deposition for total N, NO_y, and NH_x. Some consistencies in the spatial patterns across total N, NO_y and NH_x deposition are apparent, but some important differences are also observable. Areas with high forest cover such as northern South America,

central Africa and the boreal forest of Russia have the lowest ratios for both NO_y and NH_x since the grid value is dominated by the forest deposition. For total deposition, the forest/grid ratio in the temperature forest of China is about 1.5 while the ratio is higher (2–5) when only dry deposition is considered. Another noticeable feature can be found in the areas in Fig. 6 with a ratio for NO_y deposition of about 2. These areas are most apparent at the edges of the denser forest cover in central Africa, India/Nepal, and north-eastern China which are areas with forest coverage less than 10%. These areas at the edge of the dense forests are less pronounced for NH_x deposition while areas in Europe have higher ratios for NH_x deposition than NO_y deposition indicating a greater difference between the grid-based deposition and the forest-specific deposition in Europe. Similar to total deposition, there are some grid cells where the ratio is less than 1 in Canada, South America, and Africa. Also in Brazil, the ratios for NH_x are much lower than for NO_y. The lower ratios of forest/grid deposition for NHx compared to NO_y are due to the differences in deposition pathways. Similar to Wesely (1989), EMEP deposition rates depend upon how water-soluble or reactive the gases are. Many NO_y compounds (especially NO_2) are not very water-soluble, and deposition is driven by stomatal uptake which is linked to reactivity, rather than non-stomatal uptake. NH_3 on the other hand is very water soluble, and deposits easily to water and humid surfaces. In grids with substantial water surfaces the grid-average NH_3 deposition can easily exceed deposition rates to forests. In general, the relatively greater non-stomatal deposition of NH_x compared to NO_y smooths out the deposition rates across different ecosystems. Results from these analyses show the importance of considering the use forest-specific deposition values in place of grid-average values in ecosystem assessments.

4. Conclusions and future research needs

Measurements of N deposition to global forest ecosystems are not readily available. Additionally, measurements are not always comparable across networks. Estimates from atmospheric models allow us to examine the deposition globally and attribute the deposition to wet or dry deposition and oxidized or reduced N deposition. Results from this study showed high spatial variability of deposition to different forest biomes. Total reactive N deposition is high for forests in China, Japan, Eastern U.S. and Europe. Asian forests received the highest level of total N deposition (Table S1), which is consistent with a recent synthesis of total N deposition in throughfall and stemflow across 33 forested sites (21.6, ranging 15.0–31.2 kg N ha^{-1} yr^{-1}) (Du et al., 2016). These deposition values include the contribution of both wet and dry deposition and also reflect the impact of large contributions from anthropogenic emissions of NO_x and NH_3. Considering only dry deposition, land use specific parameters such as LAI are major controlling factors. Our results show that dry deposition contributes more to total deposition for forests in tropical areas due to their high LAI and long growing season. Spatial differences in the relative contributions of NH_x and NO_y to total N deposition to forests reflect a combination of effects of emissions, meteorology, and deposition processes.

To date, most studies that have examined deposition to forests have used grid-based values rather than forest-specific values. This study shows that for global forests that are in areas where the grid cell is not predominantly forested, deposition estimates may be a factor of 2 or more higher in grid squares with significant non-forest fraction if the forest-specific deposition is used and is on average 12% higher for all global forests. Differences of that magnitude could have an impact on the determination of critical load exceedance for forest biomes. Therefore, our results suggest that the use of land use specific deposition values is important for ecological assessments. Few models include this output routinely, but providing land use specific deposition along with landcover information would provide information to improve the understanding of the differences between model predictions of deposition. We also note that this publication did not consider sub-grid heterogeneity in wet deposition over forests and other surfaces. Especially in terrains with heterogeneous orography, sloped hills may be less suitable for agriculture and be covered by forests, while they can also be subject to different precipitation patterns depending on dominant weather patterns. This publication also did not assess the possible interaction of sub-grid emission variability and deposition to forests, which can be especially important for forests embedded in agricultural regions. Higher spatial resolution, 'forest-resolving' models will be better equipped to calculate deposition to forests.

It is important to note that currently available model parametrizations have been based on a small number of direct deposition or process-level field studies over a limited number of land covers and forest types. The models have been extended to represent all forest biomes, but the specification of needed parameters to drive the models is uncertain. Additional measurements, for example, of critical gaseous species such as NH_3 and HNO_3, as well as of deposition rates, are needed to verify the models and the observed temporal and spatial patterns. Further studies to improve the understanding of organic nitrates are also important for characterizing the N budget, particularly in forests given the importance of the interaction of biogenic emissions with NO_x. Also, meteorological and air quality models use a variety of land use coverages and assumptions on LAI and phenology to drive the characterization of the surface fluxes. The impact of the choice of land use coverage has not been assessed and could be very important for combining model output to create ensemble values which are more commonly being developed for use in ecological assessments.

Disclaimer

The views expressed in this article are those of the authors and do not necessarily represent the views or policies of the U.S. Environmental Protection Agency.

Acknowledgement

The EMEP work was funded by EMEP under UNECE, with computer time supported by the Research Council of Norway (Programme for Supercomputing). We acknowledge Jan Cees Voogd of Wageningen University and Research for producing the maps of the HTAP2 and EMEP model results. This paper benefitted from discussions at the WMO MMF-GTAD workshop in 2017. The authors thank the HTAP2 modellers for their model simulations. FD acknowledges the H2020 VERIFY project for support. Data used in this study are available at http://thredds.met.no/thredds/catalog/data/EMEP/Articles_data/Schwede_etal_Ndep_2018/catalog.html.

Appendix A. Supplementary data

Supplementary data to this article can be found online at https://doi.org/10.1016/j.envpol.2018.09.084.

References

Aber, J., McDowell, W., Nadelhoffer, K., Magill, A., Berntson, G., Kamakea, M., McNulty, S., Currie, W., Rustad, L., Fernandez, I., 1998. Nitrogen saturation in temperate forest ecosystems: hypotheses revisited. BioScience 48, 921–934.

Appel, K.W., Napelenok, S.L., Foley, K.M., Pye, H.O.T., Hogrefe, C., Luecken, D.J., Bash, J.O., Roselle, S.J., Pleim, J.E., Foroutan, H., Hutzell, W.T., Pouliot, G.A., Sarwar, G., Fahey, K.M., Gantt, B., Gilliam, R.C., Heath, N.K., Kang, D., Mathur, R., Schwede, D.B., Spero, T.L., Wong, D.C., Young, J.O., 2017. Description and

evaluation of the community Multiscale air quality (CMAQ) modeling system version 5.1. Geosci. Model Dev. 10, 1703–1732.
Bash, J.O., Cooter, E.J., Dennis, R.L., Walker, J.T., Pleim, J.E., 2013. Evaluation of a regional air-quality model with bidirectional NH_3 exchange coupled to an agroecosystem model. Biogeosciences 10, 1635–1645.
Bey, I., Jacob, D.J., Yantosca, R.M., Logan, J.A., Field, B., Fiore, A.M., Li, Q., Liu, H., Mickley, L.J., Schultz, M., 2001. Global modeling of tropospheric chemistry with assimilated meteorology: model description and evaluation. J. Geophys. Res. 106, 23,073-23,096.
Bowman, W.D., Cleveland, C.C., Halada, L., Hresko, J., Baron, J., 2008. Negative impact of nitrogen deposition on soil buffering capacity. Nat. Geosci. 1, 767–770.
Britto, D.T., Kronzucker, H.J., 2002. NH_4^+ toxicity in higher plants: a critical review. J. Plant Physiol. 159 (6), 567–584.
Britto, D.T., Kronzucker, H.J., 2013. Ecological significance and complexity of n-source preference in plants. Ann. Bot. 112 (6), 957–963.
Cape, J.N., Cornell, S.E., Jickells, T.D., Nemitz, E., 2011. Organic nitrogen in the atmosphere — where does it come from? A review of sources and methods. Atmos. Res. 102, 30–48.
Chin, M., Rood, R.B., Lin, S.-J., Müller, J.-F., Thompson, A.M., 2000. Atmospheric sulfur cycle simulated in the global model GOCART: model description and global properties. J. Geophys. Res. Atmos. 105, 24671–24687. https://doi.org/10.1029/2000JD900384.
Colarco, P., da Silva, A., Chin, M., Diehl, T., 2010. Online simulations of global aerosol distributions in the NASA GEOS-4 model and comparisons to satellite and ground-based aerosol optical depth. J. Geophys. Res. Atmos. 115, D14207. https://doi.org/10.1029/2009JD012820.
Cornell, S.E., Jickells, T.D., Cape, J.N., Rowland, A.P., Duce, R.A., 2003. Organic nitrogen deposition on land and coastal environments: a review of methods and data. Atmos. Environ. 37, 2173–2191.
Cornell, S.E., 2011. Atmospheric nitrogen deposition: revisiting the question of the importance of the organic component. Environ. Pollut. 159, 2214–2222.
Dentener, F., Drevet, J., Lamarque, J.F., Bey, I., Eickhout, B., Fiore, A.M., Hauglustaine, D., Horowitz, L.W., Krol, M., Kulshrestha, U.C., Lawrence, M., Galy-Lacaux, C., Rast, S., Shindell, D., Stevenson, D., Van Noije, T., Atherton, C., Bell, N., Bergman, D., Butler, T., Cofala, J., Collins, B., Doherty, R., Ellingsen, K., Galloway, J., Gauss, M., Montanaro, V., Müller, J.F., Pitari, G., Rodriguez, J., Sanderson, M., Solmon, F., Strahan, S., Schultz, M., Sudo, K., Szopa, S., Wild, O., 2006. Nitrogen and sulfur deposition on regional and global scales: a multimodel evaluation. Global Biogeochem. Cy. 20, GB4003.
Dentener, F.R., Vet, R., Dennis, L., Du, E., Kulshrestha, U.C., Galy-Lacaux, C., 2014. Progress in monitoring and modelling estimates of nitrogen deposition at local, regional and global scales. In: Nitrogen Deposition, Critical Loads and Biodiversity. Springer Netherlands, pp. 7–22.
De Vries, W., Reinds, G.J., Gundersen, P., Sterba, H., 2006. The impact of nitrogen deposition on carbon sequestration in European forests and forest soils. Global Change Biol. 12, 1151–1173.
De Vries, W., Du, E., Butterbach-Bahl, K., 2014a. Short and long-term impacts of nitrogen deposition on carbon sequestration by forest ecosystems. Curr. Opin. Env. Sust. 9, 90–104.
De Vries, W., Dobbertin, M.H., Solberg, S., van Dobben, H.F., Schaub, M., 2014b. Impacts of acid deposition, ozone exposure and weather conditions on forest ecosystems in Europe: an overview. Plant Soil 380, 1–45.
Dirnböck, T., Grandin, U., Romermann, M.B., Beudert, B., Canullo, R., Forsius, M., Grabner, M.-T., Holmberg, M., Kleemola, S., Lundin, L., Mirtl, M., Neumann, M., Pompei, E., Salemaa, M., Starlinger, F., Staszewski, T., Uziębło, A.K., 2014. Forest floor vegetation response to nitrogen deposition in Europe. Global Change Biol. 20, 429–440.
Du, E., Fang, J., 2014. Weak growth response to nitrogen deposition in an old-growth boreal forest. Ecosphere 5 (9), art109.
Du, E., Jiang, Y., Fang, J., De Vries, W., 2014a. Inorganic nitrogen deposition in China's forests: status and characteristics. Atmos. Environ. 98, 474–482.
Du, E., De Vries, W., Galloway, J., Hu, X., Fang, J., 2014b. Changes in wet nitrogen deposition in the United States between 1985 and 2012. Environ. Res. Lett. 9, 095004.
Du, E., De Vries, W., Han, W., Liu, X., Yan, Z., Jiang, Y., 2016. Imbalanced phosphorus and nitrogen deposition in China's forests. Atmos. Chem. Phys. 16 (13), 8571–8579.
Du, E., 2016. Rise and fall of nitrogen deposition in the United States. P. Natl. Acad. Sci. USA 113 (26), E3594–E3595.
Du, E., De Vries, W., 2018. Nitrogen-induced new net primary production and carbon sequestration in global forests. Environ. Pollut. https://doi.org/10.1016/j.envpol.2018.08.041.
Emberson, L., Ashmore, M., Simpson, D., Tuovinen, J.-P., Cambridge, H., 2001. Modelling and mapping ozone deposition in Europe water air. Soil Pollut. 130, 577–582.
Environment and Climate Change Canada, 2018. Atmospheric Deposition Analysis generated by Optimal Interpolation from Observations. https://open.canada.ca/ckan/en/dataset/4403f5af-e598-5a43-802f-c14c8538a21f. (Accessed 31 March 2018).
Fahey, K.M., Carlton, A.G., Pye, H.O.T., Baek, J., Hutzell, W.T., Stanier, C.O., Baker, K.R., Appel, K.W., Jaoui, M., Offenberg, J.H., 2017. A framework for expanding aqueous chemistry in the Community Multiscale Air Quality (CMAQ) model version 5.1. Geosci. Model Dev. 10, 1587–1605.
Flechard, C.R., Nemitz, E., Smith, R.I., Fowler, D., Vermeulen, A.T., Bleeker, A., Erisman, J.W., Simpson, D., Zhang, L., Tang, Y.S., Sutton, M.A., 2011. Dry deposition of reactive nitrogen to European ecosystems: a comparison of inferential models across the NitroEurope network. Atmos. Chem. Phys. 11, 2703–2728.
Flemming, J., Huijnen, V., Arteta, J., Bechtold, P., Beljaars, A., Blechschmidt, A.-M., Diamantakis, M., Engelen, R.J., Gaudel, A., Inness, A., Jones, L., Josse, B., Katragkou, E., Marecal, V., Peuch, V.-H., Richter, A., Schultz, M.G., Stein, O., Tsikerdekis, A., 2015. Tropospheric chemistry in the integrated forecasting system of ECMWF. Geosci. Model Dev. 8, 975–1003. https://doi.org/10.5194/gmd-8-975-2015.
Fowler, D., Pilegaard, K., Sutton, M.A., Ambus, P., Raivonen, M., Duyzer, J., Simpson, D., Fagerli, H., Fuzzi, S., Schjoerring, J.K., Granier, C., Neftel, A., Isaksen, I.S.A., Laj, P., Maione, M., Monks, P.S., Burkhardt, J., Daemmgen, U., Neirynck, J., Personne, E., Wichink-Kruit, R., Butterbach-Bahl, K., Flechard, C., Tuovinen, J.P., Coyle, M., Gerosa, G., Loubet, B., Altimir, N., Gruenhage, L., Ammann, C., Cieslik, S., Paoletti, E., Mikkelsen, T.N., Ro-Poulsen, H., Cellier, P., Cape, J.N., Horváth, L., Loreto, F., Niinemets, Ü., Palmer, P.I., Rinne, J., Misztal, P., Nemitz, E., Nilsson, D., Pryor, S., Gallagher, M.W., Vesala, T., Skiba, U., Brüggemann, N., Zechmeister-Boltenstern, S., Williams, J., O'Dowd, C., Facchini, M.C., de Leeuw, G., Flossman, A., Chaumerliac, N., Erisman, J.W., 2009. Atmospheric composition change: ecosystems–Atmosphere interactions. Atmos. Environ. 43, 5193–5267.
Galloway, J.N., Dentener, F.J., Capone, D.G., Boyer, E.W., Howarth, R.W., Seitzinger, S.P., Asner, G.P., Cleveland, C.C., Greene, P.A., Holland, E.A., Karl, D.M., Michaels, A.F., Porter, J.H., Townsend, A.R., Vörösmarty, C.J., 2004. Nitrogen cycles: past, present and future. Biogeochemistry 70 (2), 153–226.
Galloway, J.N., Townsend, A.R., Erisman, J.W., Bekunda, M., Cai, Z., Freney, J.R., Martinelli, L.A., Seitzinger, S.P., Sutton, M.A., 2008. Transformation of the nitrogen cycle: recent trends, questions, and potential solutions. Science 320 (5878), 889–892.
Galmarini, S., Koffi, B., Solazzo, E., Keating, T., Hogrefe, C., Schulz, M., Benedictow, A., Griesfeller, J.J., Janssens-Maenhout, G., Carmichael, G., Fu, J., Dentener, F., 2017. Technical note: coordination and harmonization of the multi-scale, multi-model activities HTAP2, AQMEII3, and MICS-Asia3: simulations, emission inventories, boundary conditions, and model output formats. Atmos. Chem. Phys. 17, 1543–1555.
Hansen, K., Sorensen, L.L., Hertel, O., Geels, C., Skjoth, C.A., Jensen, B., Boegh, E., 2013. Ammonia emissions from deciduous forest after leaf fall. Biogeosciences 10, 4577–4589. https://doi.org/10.5194/bg-10-4577-2013.
Hansen, M., Stehman, S., Potapov, P., 2010. Quantification of global gross forest cover loss. PNAS 107 (19), 8650–8655.
Hedin, L., Brookshire, E., Menge, D., Barron, A., 2009. The nitrogen paradox in tropical forest ecosystems. Annu. Rev. Ecol. Evol. Syst. 40, 613–645.
Henze, D.K., Hakami, A., Seinfeld, J.H., 2007. Development of the adjoint of GEOS-Chem. Atmos. Chem. Phys. 7, 2413–2433. https://doi.org/10.5194/acp-7-2413-2007.
Högberg, P., 2012. What is the quantitative relation between N deposition and forest carbon sequestration? Global Change Biol. 18, 1–2.
Janssens-Maenhout, G., Crippa, M., Guizzardi, D., Dentener, F., Muntean, M., Pouliot, G., Keating, T., Zhang, Q., Kurokawa, J., Wankmüller, R., Denier van der Gon, H., Kuenen, J.J.P., Klimont, Z., Frost, G., Darras, S., Koffi, B., Li, M., 2015. HTAP_v2.2: a mosaic of regional and global emission grid maps for 2008 and 2010 to study hemispheric transport of air pollution. Atmos. Chem. Phys. 15, 11411–11432.
Jarvis, P.G., 1976. The Interpretation of the variations in leaf water potential and stomatal conductance found in canopies in the field. P Roy. Soc. B-Biol. Sci. 273, 593–610.
Jia, Y., Yu, G., Gao, Y., He, N., Wang, Q., Jiao, C., Zuo, Y., 2016. Global inorganic nitrogen dry deposition inferred from ground- and space-based measurements. Sci. Rep. 6, 19810.
Jiang, Z., McDonald, B.C., Worden, H., Worden, J.R., Miyazaki, K., Qu, Z., Henze, D.K., Jones, D.B.A., Arellano, A.F., Fischer, E.V., Zhu, L., Boersma, K.F., 2018. Unexpected slowdown of US pollutant emission reduction in the past decade. PNAS. https://www.pnas.org/cgi/doi/10.1073/pnas.1801191115.
Jickells, T., Baker, A.R., Cape, J.N., Cornell, S.E., Nemitz, E., 2013. The cycling of organic nitrogen through the atmosphere. P Roy. Soc. B-Biol. Sci. 368, 20130115. https://doi.org/10.1098/rstb.2013.0115.
Kanakidou, M., Duce, R.A., Prospero, J.M., Baker, A.R., Benitez-Nelson, C., Dentener, F.J., Hunter, K.A., Liss, P.S., Mahowald, N., Okin, G.S., Sarin, M., Tsigaridis, K., Uematsu, M., Zamora, L.M., Zhu, T., 2012. Atmospheric fluxes of organic N and P to the global ocean. Global Biogeochem. Cy. 26 (3), GB3026. https://doi.org/10.1029/2011GB004277.
Kanakidou, M., Myriokefalitakis, S., Daskalakis, N., Fanourgakis, G., Nenes, A., Baker, A.R., Tsigaridis, K., Mihalopoulos, N., 2016. Past, present, and future atmospheric nitrogen deposition. J. Atmos. Sci. 73, 2039–2047.
Keenan, R.J., Reams, G.A., Achard, F., Freitas, J.V.D., Grainger, A., Lindquist, E., 2015. Dynamics of global forest area: results from the FAO global forest resources assessment 2015. Forest Ecol. Manag. 352, 9–20.
Khan, T.R., Perlinger, J.A., 2017. Evaluation of five dry particle deposition parameterizations for incorporation into atmospheric transport models. Geosci. Model Dev. 10, 3861–3888.
Kharol, S.K., Shephard, M.W., McLinden, C.A., Zhang, L., Sioris, C.E., O'Brien, J.M., Vet, R., Cady-Pereira, K.E., Hare, E., Siemons, J., Krotkov, N.A., 2018. Dry Deposition of reactive nitrogen from satellite observations of ammonia and nitrogen dioxide over North America. Environ. Res. Lett. 45, 1157–1166.
Klimont, Z., Kupiainen, K., Heyes, C., Purohit, P., Cofala, J., Rafaj, P., Borken-

Kleefeld, J., Schöpp, W., 2017. Global anthropogenic emissions of particulate matter including black carbon. Atmos. Chem. Phys. 17, 8681–8723. https://doi.org/10.5194/acp-17-8681-2017.

Kouznetsov, R., Sofiev, M., 2012. A methodology for evaluation of vertical dispersion and dry deposition of atmospheric aerosols. J. Geophys. Res. Atmos. 117, D1. https://doi.org/10.1029/2011JD016366.

Lamarque, J.F., Dentener, F., Mcconnell, J., Ro, C.U., Shaw, M., Ve4, R., Bergmann, D., Cameron-Smith, P., Dalsoren, S., Doherty, R., Faluvegi, G., Ghan, S.J., Josse, B., Lee, Y.H., MacKenzie, I.A., Plummer, D., Shindell, D.T., Skeie, R.B., Stevenson, D.S., Strode, S., Zeng, G., Curran, M., Dahl-Jensen, D., Das, S., Fritzsche, D., Nolan, M., 2013. Multi-model mean nitrogen and sulfur deposition from the Atmospheric Chemistry and Climate Model Intercomparison Project (ACCMIP): evaluation historical and projected changes. Atmos. Chem. Phys. 13 (16), 7997–8018.

Liu, X., Zhang, Y., Han, W., Tang, A., Shen, J., Cui, Z., Vitousek, P., Erisman, J., Goulding, K., Christie, P., Fangmeier, A., Zhang, F., 2013. Enhanced nitrogen deposition over China. Nature 494, 459–462.

Massad, R.S., Nemitz, E., Sutton, M.A., 2010. Review and parameterisation of bi-directional ammonia exchange between vegetation and the atmosphere. Atmos. Chem. Phys. 10, 10359–10386.

Mills, G., Sharps, K., Simpson, D., Pleijel, H., Broberg, M., Uddling, J., Jaramillo, F., Davies William, J., Dentener, F., Berg, M., Agrawal, M., Agrawal, S., Ainsworth, E.A., Büker, P., Emberson, L., Feng, Z., Harmens, H., Hayes, F., Kobayashi, K., Paoletti, E., Dingenen, R., 2018. Ozone pollution will compromise efforts to increase global wheat production. Glob. Change Biol. 24, 3560–3574.

Moran, M.D., Ménard, S., Talbot, D., Huang, P., Makar, P.A., Gong, W., Landry, H., Gravel, S., Gong, S., Crevier, L.-P., Kallaur, A., Sassi, M., 2010. Particulate-matter forecasting with GEM-MACH15, a new Canadian air-quality forecast model. In: Steyn, D.G., Rao, S.T. (Eds.), Air Pollution Modelling and It's Application XX. Springer, Dordrecht, pp. 289–292.

Neff, J.C., Holland, E.A., Dentener, F., McDowell, W.H., Russell, K.M., 2002. The origin, composition and rates of organic nitrogen deposition: a missing piece of the nitrogen cycle? Biogeochemistry 57–58, 99–136.

Ng, N.L., Brown, S.S., Archibald, A.T., Atlas, E., Cohen, R.C., Crowley, J.N., Day, D.A., Donahue, N.M., Fry, J.L., Fuchs, H., Griffin, R.J., Guzman, M.I., Herrmann, H., Hodzic, A., Iinuma, Y., Jimenez, J.L., Kiendler-Scharr, A., Lee, B.H., Luecken, D.J., Mao, J., McLaren, R., Mutzel, A., Osthoff, H.D., Ouyang, B., Picquet-Varrault, B., Platt, U., Pye, H.O.T., Rudich, Y., Schwantes, R.H., Shiraiwa, M., Stutz, J., Thornton, J.A., Tilgner, A., Williams, B.J., Zaveri, R.A., 2017. Nitrate radicals and biogenic volatile organic compounds: oxidation, mechanisms, and organic aerosol. Atmos. Chem. Phys. 17, 2103–2162.

Nordin, A., Strengbom, J., Ericson, L., 2006. Responses to ammonium and nitrate additions by boreal plants and their natural enemies. Environ. Pollut. 141, 167–174.

Oleson, K., Lawrence, D., Bonan, G., Flanner, M., Kluzek, E., Lawrence, P., Levis, S., Swenson, S., Thornton, P., Dai, A., Decker, M., Dickinson, R., Feddema, J., Heald, C., Hoffman, F., Lamarque, J., Mahowald, N., Niu, G., Qian, T., Randerson, J., Running, S., Sakaguchi, K., Slater, A., Stockli, R., Wang, A., Yang, Z., Zeng, X., Zeng, X., 2010. Technical Description of Version 4.0 of the Community Land Model (CLM), NCAR Technical Note NCAR/TN-478+STR. National Center for Atmospheric Research, National Center for Atmospheric Research, Boulder, CO.

Petroff, A., Mailliat, A., Amielh, M., Anselmet, F., 2008a. Aerosol dry deposition on vegetative canopies. Part I: review of present knowledge. Atmos. Environ. 42, 3625–3653.

Petroff, A., Mailliat, A., Amielh, M., Anselmet, F., 2008b. Aerosol dry deposition on vegetative canopies. Part II: a new modelling approach and applications. Atmos. Environ. 42, 3654–3683.

Petroff, A., Zhang, L., 2010. Development and validation of a size-resolved particle dry deposition scheme for application in aerosol transport models. Geosci. Model Dev. 3, 753–769.

Pleim, J., Ran, L., 2011. Surface flux modeling for air quality applications. Atmosphere 2, 271–302.

Pryor, S.C., Gallagher, M., Sievering, H., Larsen, S.E., Barthelmie, R.J., Birsan, F., Nemitz, E., Rinne, J., Kulmala, M., Groenholm, T., Taipale, R., Vesala, T., 2008. A review of measurement and modelling results of particle atmosphere-surface exchange. Tellus Ser. B Chem. Phys. Meteorol. 60, 42–75.

Pye, H.O., Luecken, D.J., Xu, L., Boyd, C.M., Ng, N.L., Baker, K.R., Ayres, B.R., Bash, J.O., Baumann, K., Carter, W.P., Edgerton, E., Fry, J.L., Hutzell, W.T., Schwede, D.B., Shepson, P.B., 2015. Modeling the current and future roles of particulate organic nitrates in the southeastern United States. Environ. Sci. Technol. 49, 14195–14203.

Rienecker, M.M., Suarez, M.J., Todling, R., Bacmeister, J., Takacs, L., Liu, H.-C., Gu, W., Sienkiewicz, M., Koster, R.D., Gelaro, R., Stajner, I., Nielsen, J.E., 2008. The GEOS-5 Data Assimilation System – Documentation of Versions 5.0.1, 5.1.0, and 5.2.0, NASA, Publication Series: NASA/TM; 2008-104606, Technical Report Series on Global Modeling and Data Assimilation, vol 27.

Sander, R., 2015. Compilation of Henry's law constants (version 4.0) for water as solvent. Atmos. Chem. Phys. 15, 4399–4981.

Schulte-Uebbing, L., De Vries, W., 2018. Global-scale impacts of nitrogen deposition on tree carbon sequestration in tropical, temperate, and boreal forests: a meta-analysis. Global Change Biol. 24 (2), e416–e431.

Schwede, D.B., Lear, G.G., 2014. A novel hybrid approach for estimating total deposition in the United States. Atmos. Environ. 92, 207–220.

Seidling, W., Fischer, R., Granke, O., 2008. Relationships between forest floor vegetation on ICP Forests monitoring plots in Europe and basic variables in soil and nitrogen deposition. Int. J. Environ. Stud. 65, 309–320.

Simpson, D., Butterbach-Bahl, K., Fagerli, H., Kesik, M., Skiba, U., Tang, S., 2006. Deposition and emissions of reactive nitrogen over European forests: a modelling study. Atmos. Environ. 40, 5712–5726.

Simpson, D., Benedictow, A., Berge, H., Bergström, R., Emberson, L.D., Fagerli, H., Flechard, C.R., Hayman, G.D., Gauss, M., Jonson, J.E., Jenkin, M.E., Nyíri, A., Richter, C., Semeena, V.S., Tsyro, S., Tuovinen, J.P., Valdebenito, Á., Wind, P., 2012. The EMEP MSC-W chemical transport model – technical description. Atmos. Chem. Phys. 12, 7825–7865.

Simpson, D., Andersson, C., Christensen, J.H., Engardt, M., Geels, C., Nyiri, A., Posch, M., Soares, J., Sofiev, M., Wind, P., Langner, J., 2014. Impacts of climate and emission changes on nitrogen deposition in Europe: a multi-model study. Atmos. Chem. Phys. 14, 6995–7017.

Simpson, D., Bergström, R., Imhof, H., Wind, P., 2017. Updates to the EMEP/MSC-W Model, 2016–2017 Transboundary Particulate Matter, Photo-oxidants, Acidifying and Eutrophying Components. The Norwegian Meteorological Institute, Oslo, Norway, pp. 115–122. Status Report 1/2017. www.emep.int.

Simpson, D., Wind, P., Bergström, R., Gauss, M., Tsyro, S., Valdebenito, A., 2018. Updates to the EMEP/MSC-W Model, 2017–2019 Transboundary Particulate Matter, Photo-oxidants, Acidifying and Eutrophying Components. The Norwegian Meteorological Institute, Oslo, Norway, pp. 109–116. Status Report 1/2018. www.emep.int.

Skrindo, A., Økland, R.H., 2002. Effects of fertilization on understorey vegetation in a Norwegian Pinus sylvestris forest. Appl. Veg. Sci. 5, 167–172.

Slinn, W.G.N., 1982. Predictions for particle deposition to vegetative canopies. Atmos. Environ. 16, 1785–1794.

Søvde, O.A., Prather, M.J., Isaksen, I.S.A., Berntsen, T.K., Stordal, F., Zhu, X., Holmes, C.D., Hsu, J., 2012. The chemical transport model Oslo CTM3. Geosci. Model Dev. 5, 1441–1469. https://doi.org/10.5194/gmd-5-1441-2012.

Stadtler, S., Simpson, D., Schröder, S., Taraborrelli, D., Bott, A., Schultz, M., 2018. Ozone impacts of gas-aerosol uptake in global chemistry-transport models. Atmos. Chem. Phys. 18, 3147–3171.

Stjern, C.W., Samset, B.H., Myhre, G., Bian, H., Chin, M., Davila, Y., Dentener, F., Emmons, L., Flemming, J., Haslerud, A.S., Henze, D., Jonson, J.E., Kucsera, T., Lund, M.T., Schulz, M., Sudo, K., Takemura, T., Tilmes, S., 2016. Global and regional radiative forcing from 20 % reductions in BC, OC and SO4 – an HTAP2 multi-model study. Atmos. Chem. Phys. 16, 13579–13599. https://doi.org/10.5194/acp-16-13579-2016.

Strengbom, J., Walheim, M., Näsholm, T., Ericson, L., 2003. Regional differences in the occurrence of understorey species reflect nitrogen deposition in Swedish forests. Ambio 32, 91–97.

Sudo, K., Takahashi, M., Kurokawa, J., Akimoto, H., 2002. CHASER: a global chemical model of the troposphere, 1. Model description. J. Geophys. Res. 107 (D17), 4339. https://doi.org/10.1029/2001JD001113.

Sutton, M.A., Simpson, D., Levy, P.E., Smith, R.I., Reis, S., van Oijen, M., De Vries, W., 2008. Uncertainties in the relationship between atmospheric nitrogen deposition and forest carbon sequestration. Global Change Biol. 14, 2057–2063.

Takemura, T., Nozawa, T., Emori, S., Nakajima, T.Y., Nakajima, T., 2005. Simulation of climate response to aerosol direct and indirect effects with aerosol transport-radiation model. J. Geophys. Res. Atmos. 110, D02202. https://doi.org/10.1029/2004JD005029.

Tan, J., Fu, J.S., Dentener, F., Sun, J., Emmons, L., Tilmes, S., Sudo, K., Flemming, J., Jonson, J.E., Gravel, S., Bian, H., Henze, D., Lund, M.T., Kucsera, T., Takemura, T., Keating, T., 2018. Multi-model study of HTAP II on sulphur and nitrogen deposition. Atmos. Chem. Phys. 18, 6847–6866.

Tilmes, S., Lamarque, J.-F., Emmons, L.K., Kinnison, D.E., Marsh, D., Garcia, R.R., Smith, A.K., Neely, R.R., Conley, A., Vitt, F., Val Martin, M., Tanimoto, H., Simpson, I., Blake, D.R., Blake, N., 2016. Representation of the community Earth system model (CESM1) CAM4-chem within the chemistry-climate model initiative (CCMI). Geosci. Model Dev. 9, 1853–1890. https://doi.org/10.5194/gmd-9-1853-2016.

Van Dobben, H.F., De Vries, W., 2010. Relation between forest vegetation, atmospheric deposition and site conditions at regional and European scales. Environ. Pollut. 158, 921–933.

Van Dobben, H.F., De Vries, W., 2017. The contribution of nitrogen deposition to the eutrophication signal in understorey plant communities of European forests. Ecol. Evol. 7, 214–227.

Val Martin, M., Heald, C.L., Arnold, S.R., 2014. Coupling dry deposition to vegetation phenology in the Community Earth System Model: implications for the simulation of surface O3. Geophys. Res. Lett. 41, 2988–2996.

Vet, R., Artz, R.S., Carou, S., Shaw, M., Ro, C.U., Aas, W., Baker, A., Bowersox, V.C., Dentener, F., Galy-Lacaux, C., Hou, A., Pienaar, J.J., Gillett, R., Forti, M.C., Gromov, S., Hara, H., Khodzher, T., Mahowald, N., Nickovic, S., Rao, P.S.P., Reid, N.W., 2014. A global assessment of precipitation chemistry and deposition of sulfur, nitrogen, sea salt, base cations, organic acids, acidity and pH, and phosphorus. Atmos. Environ. 93, 3–100.

Vivanco, M.G., Theobald, M.R., García-Gómez, H., Garrido, J.L., Prank, M., Aas, W., Adani, M., Alyuz, U., Andersson, C., Bellasio, R., Bessagnet, B., Bianconi, R., Bieser, J., Brandt, J., Briganti, G., Cappelletti, A., Curci, G., Christensen, J.H., Colette, A., Couvidat, F., Cuvelier, K., D'Isidoro, M., Flemming, J., Fraser, A., Geels, C., Hansen, K.M., Hogrefe, C., Im, U., Jorba, O., Kitwiroon, N., Manders, A., Mircea, M., Otero, N., Pay, M.T., Pozzoli, L., Solazzo, E., Tsyro, S., Unal, A., Wind, P., Galmarini, S., 2018. Modelled deposition of nitrogen and sulfur in Europe estimated by 14 air quality model-systems: evaluation, effects of changes in emissions and implications for habitat protection. Atmos. Chem. Phys. 18, 10199–10218.

Waldner, P., Marchetto, A., Thimonier, A., Schmitt, M., Rogora, M., Granke, O., Mues, V., Hansen, K., Karlsson, G.P., Zlindra, D., Clarke, N., Verstraeten, A., Lazdins, A., Schimming, C., Iacoban, C., Lindroos, A., Vanguelova, E., Benham, S., Meesenburg, H., Nicolas, M., Kowalska, A., Apuhtin, V., Napa, U., Lachmanova, Z., Kristoefel, F., Bleeker, A., Ingerslev, M., Vesterdal, L., Molina, J., Fischer, U., Seidling, W., Jonard, M., O'Dea, P., Johnson, J., Fischer, R., Lorenz, M., 2014. Detection of temporal trends in atmospheric deposition of inorganic nitrogen and sulphate to forests in Europe. Atmos. Environ. 95, 363–374.

Wang, X., Zhang, L., Moran, M.D., 2010. Uncertainty assessment of current size-resolved parameterizations for below-cloud particle scavenging by rain. Atmos. Chem. Phys. 10, 5685–5705.

Watanabe, M., Suzuki, T., O'ishi, R., Komuro, Y., Watanabe, S., Emori, S., Takemura, T., Chikira, M., Ogura, T., Sekiguchi, M., Takata, K., Yamazaki, D., Yokohata, T., Nozawa, T., Hasumi, H., Tatebe, H., Kimoto, M., 2010. Improved climate simulation by MIROC5: mean states, variability, and climate sensitivity. J. Clim. 23, 6312–6335. https://doi.org/10.1175/2010JCLI3679.1.

Wesely, M.L., 1989. Parameterization of surface resistances to gaseous dry deposition in regional-scale numerical models. Atmos. Environ. 23, 1293–1304.

Wesely, M.L., Hicks, B.B., 2000. A review of the current status of knowledge on dry deposition. Atmos. Environ. 34, 2261–2282.

Wichink Kruit, R.J., Schaap, M., Sauter, F.J., van Zanten, M.C., van Pul, W.A.J., 2012. Modeling the distribution of ammonia across Europe including bi-directional surface-atmosphere exchange. Biogeosciences 9, 5261–5277.

World Meteorological Organization, 2017. Global Atmosphere Watch Workshop on Measurement-model Fusion for Global Total Atmospheric Deposition (MMF-GTAD), 28 February – 2 March 2017, vol 234. GAW Report No, Geneva, Switzerland, p. 45.

Xu, L., Pye, H.O.T., He, J., Chen, Y., Murphy, B.N., Ng, N.L., 2018. Experimental and model estimates of the contributions from biogenic monoterpenes and sesquiterpenes to secondary organic aerosol in the southeastern United States. Atmos. Chem. Phys. 18, 12613–12637, 2018. https://doi.org/10.5194/acp-18-12613-2018.

Yang, C.-E., Mao, J., Hoffman, F.M., Ricciuto, D.M., Fu, J.S., Jones, C.D., Thurner, M., 2018. Uncertainty quantification of extratropical forest biomass in CMIP5 models over the Northern Hemisphere. Sci. Rep. 8, 10962. https://doi.org/10.1038/s41598-018-29227-7.

Zhang, L., Brook, J.R., Vet, R., 2003. A revised parameterization for gaseous dry deposition in air-quality models. Atmos. Chem. Phys. 3, 2067–2082.

Zhang, L., He, Z., 2014. Technical Note: an empirical algorithm estimating dry deposition velocity of fine, coarse and giant particles. Atmos. Chem. Phys. 14, 3729–3737.

Zhang, J., Shao, Y., 2014. A new parameterization of particle dry deposition over rough surfaces. Atmos. Chem. Phys. 14, 12429–12440.

Zhang, L., Wang, X., Moran, M.D., Feng, J., 2013. Review and uncertainty assessment of size-resolved scavenging coefficient formulations for below-cloud snow scavenging of atmospheric aerosols. Atmos. Chem. Phys. 13, 10005–10025.